ISIJ International, Vol. 47 (2007), No. 6, pp. 869–874

Microstructural Analysis of Infrared Brazed Ti–6Al–4V and Nb Using the Ti–15Cu–25Ni Foil

D. W. LIAW,[1)] Z. Y. WU,[2)] R. K. SHIUE[2)] and C. S. CHANG[3)]

1) Department of Materials Science and Engineering, National Dong Hwa University, Hualien 974, Taiwan.
2) Department of Materials Science and Engineering, National Taiwan University, Taipei 106, Taiwan.
E-mail: rkshiue@ntu.edu.tw
3) Engineered Materials Solutions, 39 Perry Avenue, MS 4-1, Attleboro, MA 02703-2410, USA.

(*Received on September 25, 2006; accepted on April 6, 2007*)

Microstructural analysis of infrared brazed Ti–6Al–4V and Nb at 970°C using the clad Ti–15Cu–25Ni filler metal has been performed in the experiment. For the 180 s brazed specimen, at first primary Ti_2Cu, Ti_2Ni as well as eutectic microstructure are obtained upon cooling cycle of brazing, and maximum amounts of Ti_2Cu and Ti_2Ni are observed at the brazed joint. The amount of transient Ti_2Cu and Ti_2Ni intermetallics is decreased with increasing the brazing time due to depletion of Cu and Ni from the braze into the Ti–6Al–4V substrate. Diffusion of Cu and Ni into Ti–6Al–4V substrate results in isothermal solidification rather than eutectic solidification of the molten braze, and the region of transformed β-Ti is broadened as the brazing time increased to 600 s and 1 200 s. For the 3 600 s brazed specimen, Ti_2Cu, Ti_2Ni and transformed β-Ti are vanished from the infrared brazed joint. Disappearance of Ti_2Cu and Ti_2Ni intermetallics for the longer brazing time makes Ti–15Cu–25Ni filler metal with a great potential in future applications.

KEY WORDS: infrared brazing; Ti–15Cu–25Ni; titanium alloy; Nb; microstructure.

1. Introduction

Titanium alloys are used for aerospace applications due to their high strength-to-weight ratio, excellent corrosion resistance and moderate creep strength. Niobium metal can be selected for its corrosion resistance in chemical and nuclear applications or for its low density and high melting point in aerospace and propulsion applications. Joining of Ti–6Al–4V and Nb has the potential application in production of missiles and rockets, because the bonding between the titanium main frame and niobium combustion chamber are required.[1)] Ag, Au and Ti-based braze alloys are possible candidates in brazing Ti–6Al–4V and Nb.[2–4)] Ag-based braze alloys are featured with low melting points, and they have been successfully applied in brazing Ti–6Al–4V and Nb metal in the previous study.[1)] Because most Ag-based braze alloys are suffered from insufficient oxidation resistance and low creep strength, they are usually not appropriate for high-temperature applications.

Most Ti alloys are difficult to be brazed with many other alloys, because high reactivity of Ti with other elements results in forming brittle interfacial intermetallics in the brazed joint so that the bonding strength is deteriorated.[5)] The Ti-based braze alloy is considered one of the most suitable fillers in brazing Ti alloys. It features low density, high corrosion resistance and moderate creep strength.[4)] However, high cost of the amorphous Ti–Cu–Ni ribbon prohibits its commercial application. The production cost of Ti–Cu–Ni foils can significantly be decreased with the aid of a cold roll-bonding process to combine Ti, Cu and Ni strips into a layered composite, so called clad Ti–Cu–Ni foils studied here.[6)]

The microstructure of Ti–Cu–Ni brazed joint is fairly complex and needs further study.[7)] In addition to solidification of the molten braze, the solid-state phase transformation of β-Ti upon cooling cycle of brazing also greatly complicates the microstructural evolution of the joint in using the Ti-based braze alloy.[7)] It is well known that the brazing condition always plays an important role in determine final microstructure of the joint. With the aid of accurate thermal cycle control, infrared heating has been proven a very powerful tool in studying the reaction kinetics of brazing.[8)] The purpose of this investigation is to extensively evaluate both microstructure and reaction sequence in the brazed joint of Ti–6Al–4V and Nb using the clad Ti–15Cu–25Ni foil.

2. Experimental Procedures

Both Ti–6Al–4V plates and Nb rods were machined into specimens with the dimension of $10\times10\times3$ mm. Clad Ti–15Cu–25Ni (wt%) foil with the total thickness of 50 μm and 50 mm wide was selected as the filler metal. The Ti–15Cu–15Ni foil was produced by a cold roll bonding process. The 0.05 mm foil consists of 7 layers arranged as Ni/Cu/Ni/Ti/Ni/Cu/Ni. The thickness of each layer was chosen so that the combined nominal composition of foil is 60 wt% Ti, 15 wt% Cu and 25 wt% Ni.

Infrared brazing was carried out in a vacuum of 5×10^{-3} Pa at 970°C for 180–3 600 s, respectively. The heating rate

of infrared brazing was kept at 10°C/s, and the average cooling rate between 570 and 1 000°C is roughly 1.3°C/s. The cross section of the brazed specimens was examined using a LEO 1530 field emission scanning electron microscope (FESEM) equipped with an energy dispersive spectrometer (EDS) with accelerating voltage of 20 kV and minimum spot size of 1 μm. Quantitative chemical analysis was performed using a JEOL JXA 8200 electron probe microanalyzer (EPMA) with a minimum spot size of 1 μm. A Rigaku RINT 2100 X-Ray diffractometer (XRD) was applied for crystal structure analysis of selected samples. The Cu Kα was chosen as the X-ray source, and its scan rate was set at 4 deg/min with the scan range between 30° and 90°. The X-ray diffraction pattern was recorded and identified based on the Powder Diffraction File (PDF).

3. Results and Discussion

Figure 1 shows the liquidus projection of Cu–Ni–Ti ternary alloy phase diagram.[9] The chemical composition of Ti–15Cu–25Ni braze alloy in atomic percent is 12.3% Cu, 22.2% Ni and balanced with Ti as marked by A in the figure. It is noted that the primitive chemical composition of molten braze alloy is hypereutectic, close to the ternary eutectic reaction, L↔Ti_2Cu+Ti_2Ni+β-Ti.[9] The molten braze initially experiences a hypereutectic reaction and results in primary Ti_2Cu and Ti_2Ni intermetallics in the joint. The solidification of residual melt subsequently yields eutectic Ti_2Cu, Ti_2Ni and β-Ti. Further cooling of the brazed joint causes eutectoid decomposition of β-Ti into the mixture of Ti_2Cu, Ti_2Ni and α-Ti. However, the morphology of transformed β-Ti is not able to be predicted from the phase diagram.

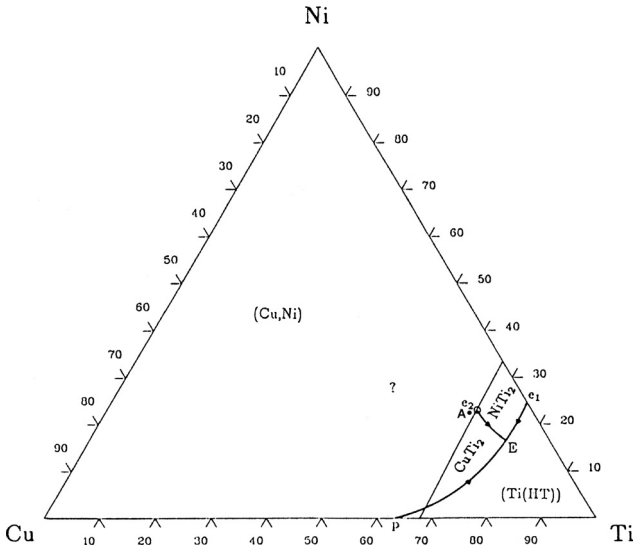

Fig. 1. The Liquidus projection of Cu–Ni–Ti ternary alloy phase diagram in atomic percent.[9]

Figure 2 displays SEM BEIs and EDS chemical analysis results of the joint infrared brazed at 970°C for 180 s. Ti_2Cu and Ti_2Ni phases cannot be clearly distinguished from the SEM backscattered electron image (BEI) and EDS chemical analysis results as illustrated in the figure. The presence of both Ti_2Cu and Ti_2Ni phases is primarily based on the following XRD structural analysis results and Cu–Ni–Ti ternary alloy phase diagrams.[9] According to Fig. 2, the joint mainly consists of Ti_2Cu, Ti_2Ni (marked by 1 and 2) and transformed β-Ti (marked by 3–5), and it is in good agreement with the Cu–Ni–Ti ternary phase diagram described above. There are different morphologies of transformed β-Ti as marked by 3–5 in Fig. 2. The microstructure morphology of transformed β-Ti depends upon both cooling rate and alloying elements of the β-Ti. Because the average cooling rate of infrared brazing is approximately kept at 1.3°C/s for all brazed specimens, the transformation of β-Ti is strongly related to redistribution of alloying elements in the β-Ti during brazing. Cu, Ni, Nb and V are β stabilizers of the Ti alloy, and Al is the only α-Ti stabilizer in the brazed joint.[10] It has been also reported that the amount of Ti_2Cu and Ti_2Ni is decreased with increasing the brazing temperature and/or time due to the depletion of Cu and Ni contents from the brazed joint.[7] For the specimen infrared brazed at 970°C for 180 s, dissolution of base metals is not prominent, so does diffusion of Cu and Ni from the molten melt into both substrates. Accordingly, the maximum amounts of Ti_2Cu and Ti_2Ni are observed at center of the joint (Fig. 2). In contrast, the transformed β-Ti is found primarily at the interface between Ti–6Al–4V and the braze alloy. According to Fig. 2, the decomposition of β-Ti upon cooling cycle results in eutectoid mixture of Ti_2Cu, Ti_2Ni and α-Ti, and it will be discussed later.

Figure 3 shows the SEM BEI of infrared brazed specimen at 970°C for 600 s. It is obvious that primary Ti_2Cu and Ti_2Ni are decreased with increasing the brazing time

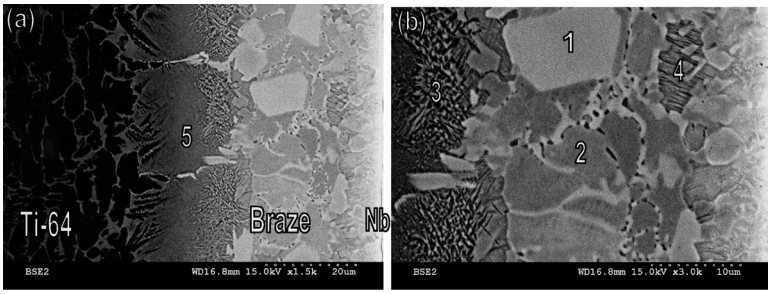

Location (phase)	Al	Nb	Ti	V	Ni	Cu
1 (Ti_2Cu,Ti_2Ni)	1.8	2.2	60.4	0.6	17.3	17.7
2 (Ti_2Cu,Ti_2Ni)	1.6	1.7	60.7	0.1	15.9	20.0
3 (transformed β-Ti)	4.5	3.5	73.0	1.4	7.5	10.1
4 (transformed β-Ti)	4.0	6.9	79.9	1.5	4.4	3.2
5 (transformed β-Ti)	7.6	2.0	77.7	2.6	5.6	4.6

Fig. 2. SEM BEIs and EDS chemical analysis results in atomic percent of the joint infrared brazed at 970°C for 180 s.

due to depletion of both Cu and Ni from the braze alloy. In contrast, the region of transformed β-Ti is increased as the brazing time increased to 600 s. Cross sections of A, B and C regions in Fig. 3 are cut and polished in order to examine microstructure of the joint at each specific area.

Figure 4 shows SEM BEI, XRD and EDS chemical analysis results of the cross section at location A in Fig. 3. According to the XRD structural analysis result, Ti_2Cu, Ti_2Ni, α-Ti and retained β-Ti are identified from the analysis. The transformed β-Ti marked by 2 and 3 in Fig. 4 stands for eutectoid decomposition of the β-Ti. Based on Cu–Ti and Ni–Ti binary alloy phase diagrams, the transformation of β-Ti yields mixture of Ti_2Ni, Ti_2Cu and α-Ti phases.[11] Additionally, the retained β-Ti stabilized by Cu, Ni and Nb contents is also identified from the XRD analysis result. It is deduced that the transformed β-Ti is comprised of non-lamellar mixture of Ti_2Cu, Ti_2Ni, α-Ti and retained β-Ti. However, the presence of actual phase(s) in the transformed β-Ti needs further study. The Nb substrate does not react with the molten braze, but it is alloyed in the β-Ti during brazing. The Nb–Ti phase diagram belongs to the β isomorphous system. Cu–Ti and Ni–Ti are categorized as the β eutectoid system.[11,12] All the elements stabilize the β phase in titanium, and accordingly, the retained β-Ti in the braze alloy is partially stabilized at room temperature due to high contents of Cu, Ni and Nb as marked by 2 and 3 (Fig. 4).

Figure 5 illustrates XRD, SEM BEIs and EDS chemical analysis results of the cross section at location B in Fig. 3.

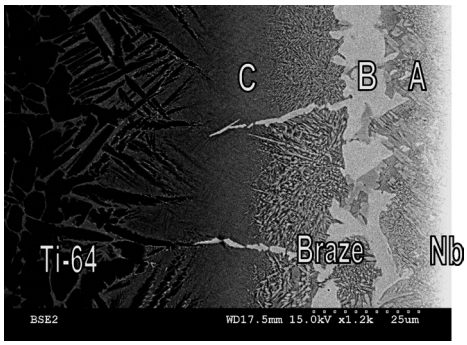

Fig. 3. The SEM BEI of the joint infrared brazed at 970° for 600 s.

The microstructure at location B is very different from that of location C. Coarse eutectic Ti_2Ni and Ti_2Cu dendrites (marked by 1) are widely observed in the figure, and the characteristic peak of Ti_2Ni is the strongest one in the XRD analysis result. The eutectic solidification of the molten braze results in Ti_2Ni, Ti_2Cu dendrites and β-Ti. Further cooling of the brazed joint after solidification causes the transformation of the β-Ti as discussed earlier. Additionally, the retained β is identified from the XRD analysis as shown in Fig. 5. Characteristic peaks of retained β-Ti at region B (Fig. 5) is less obvious than those at region A (Fig. 4) because of lower Nb content in the region B.

Figure 6 shows XRD, SEM BEIs and EDS chemical analysis results of the cross section at location C in Fig. 3. The coarse eutectic Ti_2Cu and Ti_2Ni dendrites are replaced by trivial grain boundary Ti_2Cu and Ti_2Ni intermetallics. Because the difference of atomic numbers between Cu and Ni is as low as one, Ti_2Cu and Ti_2Ni phases can not be clearly distinguished from the SEM BEI as illustrated in Fig. 6. The coexistence of both Ti_2Cu and Ti_2Ni phases is primarily demonstrated by the XRD structural analysis and Cu–Ni–Ti ternary alloy phase diagram.[9] The lack of eutectic microstructure demonstrates that solid-state interdiffusion instead of solidification dominates the metallurgical reaction at location C. The rapid grain boundary diffusion of Ni and Cu from the molten braze into Ti–6Al–4V substrate results in formation of grain boundary Ti_2Cu and Ti_2Ni. On the other hand, bulk diffusion delivers both Cu and Ni from the melt into Ti–6Al–4V substrate causing the β-Ti alloyed with Cu and Ni at the brazing temperature. The transformation of β-Ti is subsequently proceeded upon the cooling cycle of brazing as illustrated in Fig. 6.

The microstructure of transformed β-Ti marked by 1 in Fig. 6 is very different from that of Fig. 5 as marked by 2. The transformed β-Ti in Fig. 5 is originated from eutectic solidification of the molten braze, and it is alloyed with higher contents of Cu, Nb and Ni. In contrast, the transformed β-Ti in Fig. 6 is not originated from the eutectic reaction, and it is alloyed with less Cu, Nb and Ni contents, primarily *via* diffusive transport from the braze into Ti–6Al–4V substrate. A much finer eutectoid microstructure of the transformed β-Ti is observed in Fig. 6. Additionally, the α-Ti dominates the entire area as demonstrated by

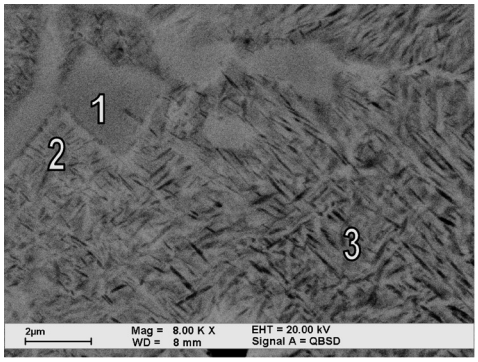

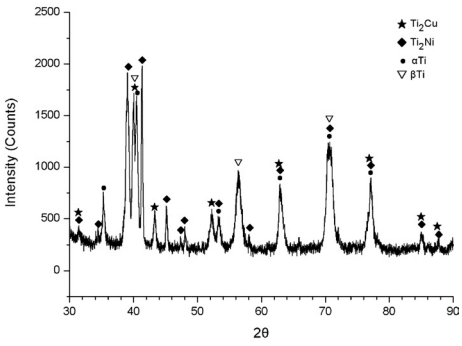

Location (phase)	Al	Nb	Ti	V	Ni	Cu
1 (Ti_2Ni, Ti_2Cu)	2.1	1.5	64.7	0.0	26.3	5.5
2 (transformed and retained β-Ti)	4.3	10.5	72.5	0.4	6.3	6.0
3 (transformed and retained β-Ti)	6.3	8.8	72.7	0.7	5.9	5.5

Fig. 4. SEM BEI, XRD and EDS chemical analysis results in atomic percent of the cross section at location A shown in Fig. 3.

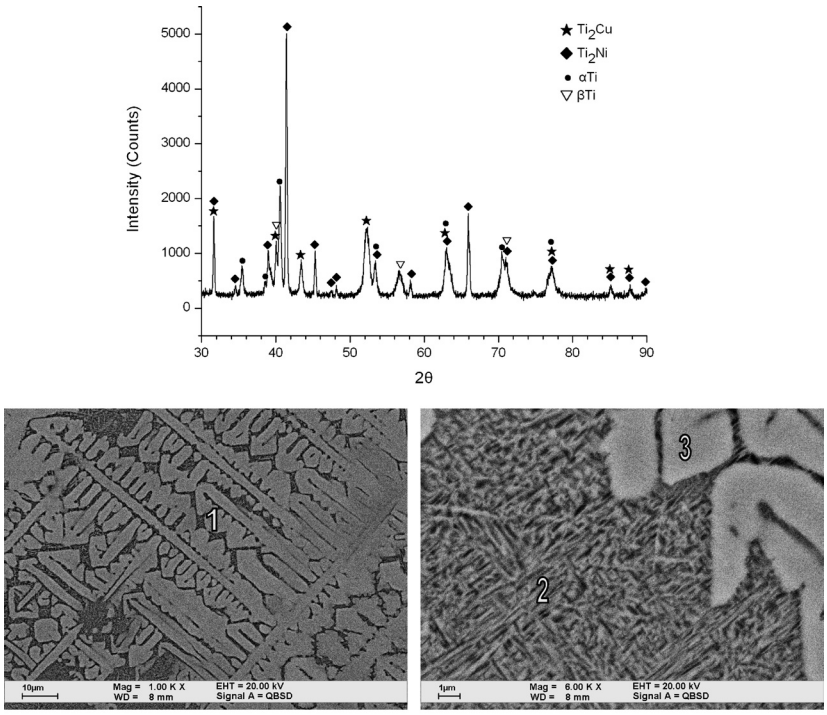

Location (phase)	Al	Nb	Ti	V	Ni	Cu
1 (Ti_2Ni, Ti_2Cu)	2.6	1.1	66.2	0.0	24.2	5.9
2 (transformed β-Ti)	5.5	4.5	75.8	0.6	7.5	6.1
3 (Ti_2Ni, Ti_2Cu)	2.2	1.5	67.2	0.0	22.8	6.3

Fig. 5. XRD, SEM BEIs and EDS chemical analysis results in atomic percent of the cross section at location B shown in Fig. 3.

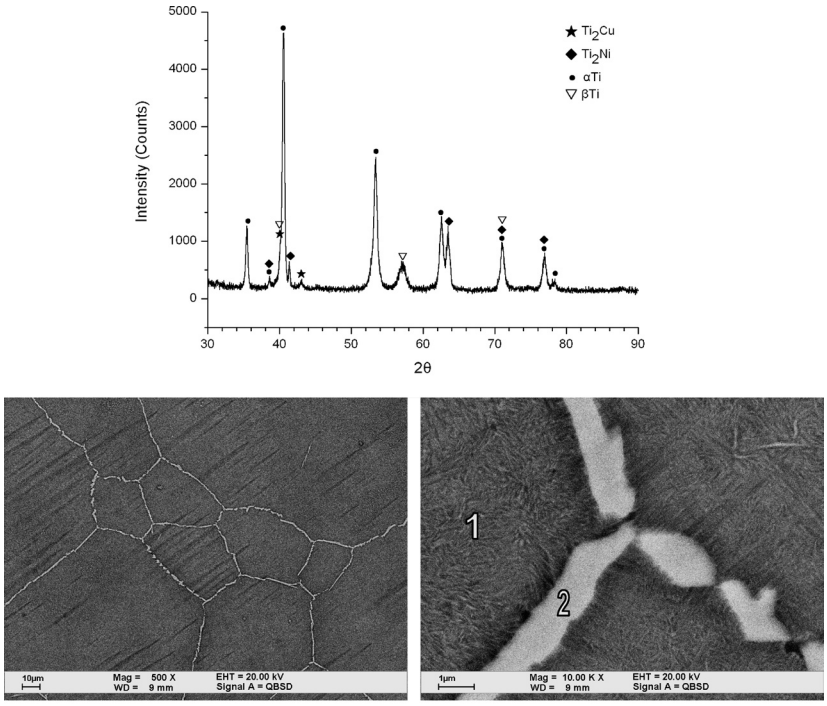

Location (phase)	Al	Nb	Ti	V	Ni	Cu
1 (transformed β-Ti)	7.8	2.9	78.5	1.3	5.4	4.2
2 (Ti_2Ni, Ti_2Cu)	4.4	1.0	66.6	0.2	22.9	4.8

Fig. 6. XRD, SEM BEIs and EDS chemical analysis results in atomic percent of the cross section at location C shown in Fig. 3.

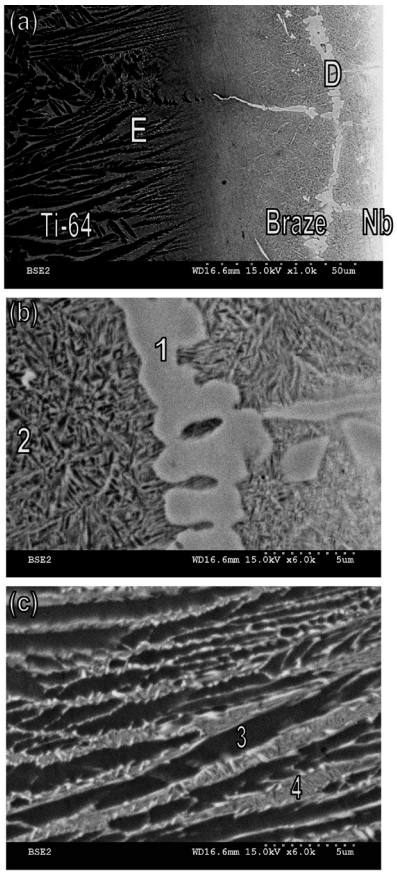

Location (phase)	Al	Nb	Ti	V	Ni	Cu
1 (Ti_2Cu,Ti_2Ni)	2.2	0.8	63.8	0.2	26.9	6.1
2 (transformed β-Ti)	3.5	5.4	77.8	1.1	6.0	6.2
3 (α-Ti)	10.4	0.0	88.3	1.0	0.1	0.1
4 (β-Ti)	6.8	0.1	79.9	5.7	5.8	1.7

Fig. 7. The SEM BEIs and EDS chemical analysis results in atomic percent of the joint infrared brazed at 970°C for 1 200 s: (a) overview of the joint, (b) higher magnification at location D and (c) higher magnification at location E.

the XRD analysis result.

Figure 7 displays the SEM BEIs and EDS chemical analysis results of the joint infrared brazed at 970°C for 1 200 s. The microstructure of Fig. 7(a) is very similar to that of Fig. 3 except for decreased eutectic Ti_2Ni and Ti_2Cu intermetallics due to depletion of Cu and Ni contents from the joint for longer brazing time. Figure 7(b) shows higher magnification at location D of Fig. 7(a). Similarly, Ti_2Cu, Ti_2Ni and transformed β-Ti are observed in the figure, and it is almost identical to Fig. 5. Figure 7(c) illustrates higher magnification at location E of Fig. 7(a). Concentrations of Nb, Cu and Ni in α-Ti and β-Ti (marked by 3 and 4 in region E) are much less than those in the transformed β-Ti (marked by 2 in region D). According to the Fig. 7(c), α-Ti is alloyed with high Al and low Cu, Nb, Ni, V, and the β-Ti is alloyed with higher contents of Cu, Ni and V.

In Figs. 3–7, regions of Ti_2Cu and Ti_2Ni may be single phase designated as $Ti_2(Cu, Ni)$. However, there is no such a $Ti_2(Cu, Ni)$ phase in the Cu–Ni–Ti ternary alloy phase diagram and the powder diffraction file.[9] Accordingly, separate Ti_2Cu and Ti_2Ni phases are proposed in the study. The TEM observation is necessary in order to locate both phases for the further study.

Figure 8(a) shows SEM BEI cross section of the joint infrared brazed at 970°C for 3 600 s. Ti_2Cu, Ti_2Ni and transformed β-Ti are completely disappeared from the joint, and they are replaced by the β-Ti as demonstrated by the XRD structural analysis (Fig. 8(d)). Figure 8(b) displays the EPMA chemical analysis results across the joint, the Nb concentration is decreased monotonously from the Nb into Ti–6Al–4V substrate. The summation of Cu and Ni concentrations in the brazed joint is approximately 5 at%, well below their original concentrations in the braze foil. The microstructure of the joint changed from β-Ti at location F (Fig. 8(c)) into mixture of α and β-Ti at location G (Fig. 8(e)). It is deduced that the stabilization of β-Ti is strongly related to the Nb concentration in these regions as demonstrated by the EPMA chemical analysis results.

Both dissolution of the Nb substrate into the molten braze and depletion of Cu as well as Ni from braze into Ti–6Al–4V increase the liquidus temperature of the molten braze. Consequently, isothermal solidification instead of eutectic solidification of the molten braze is proceeded during infrared brazing. It is unusual that the intermetallic compound in the brazed joint is vanished from the joint for the extended brazing time. In most brazing cases, the growth of stable intermetallics is usually observed for higher brazing temperature and/or longer brazing time. However, it is not the case of brazing Ti–6Al–4V and Nb using the Ti–15Cu–25Ni foil. Based on the Cu–Ti and Ni–Ti binary alloy phase diagrams, the maximum solubility of Cu and Ni in β-Ti is as high as 13.5 and 10 at%, respectively.[11] In contrast, maximum solubilities of Cu and Ni in α-Ti are 1.6 and 0.2 at%, which are much lower than those of β-Ti.[11] The chemical composition of Ti–15Cu–25Ni braze alloy in atomic percent is 12.3% Cu, 22.2% Ni and balanced with Ti. It is deduced that both Cu and Ni in the molten braze are dissolved into the β-Ti driven by concentration gradient during infrared brazing. The depletion of Cu and Ni from the molten braze into Ti–6Al–4V substrate results in disappearance of Ti_2Cu and Ti_2Ni intermetallics from the joint for longer brazing time, and it makes Ti–15Cu–25Ni filler metal with a great potential in future applications.

4. Conclusions

Microstructural evolution of infrared brazing Ti–6Al–4V and niobium metal at 970°C using the clad Ti–15Cu–25Ni foil for 180–3 600 s has been accessed in the experiment. Important conclusions are summarized below:

(1) For the 180 s brazed specimen, primary Ti_2Cu, Ti_2Ni and eutectic microstructure are obtained upon cooling cycle of brazing. Further cooling of the brazed joint results in transformation of the β-Ti. The morphology of transformed β-Ti depends on the concentration of its alloying elements such as Cu, Ni and Nb in the joint. For the short time brazed specimen, dissolution of two base metals is not prominent, so does the diffusive transport of Cu and Ni from the melt into both substrates. Accordingly, maximum amounts of Ti_2Cu and Ti_2Ni are observed at the center of joint.

(2) The amount of transient Ti_2Cu and Ti_2Ni intermetallics is decreased with increasing the brazing time due to depletion of Cu and Ni from the braze into the Ti–6Al–4V substrate. Diffusion of Cu and Ni into

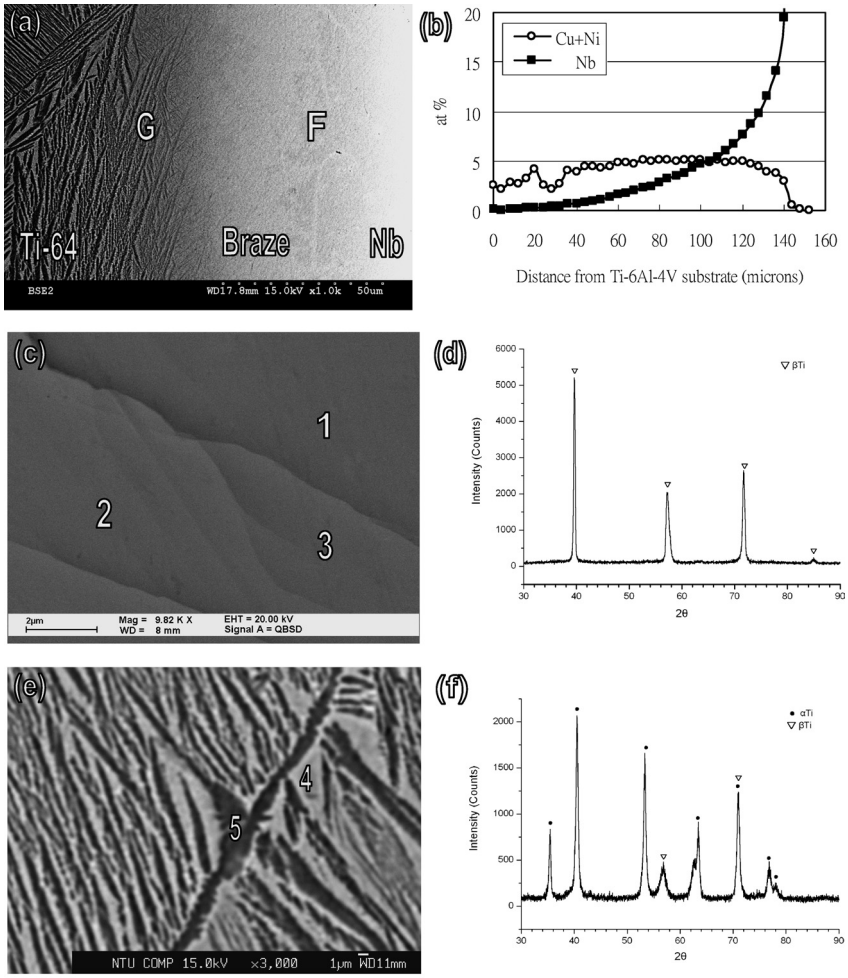

Location (phase) / at%	Al	Nb	Ti	V	Ni	Cu
1	7.8	13.5	71.0	1.1	3.4	3.1
2	7.1	16.7	69.9	0.7	3.3	2.4
3	7.5	13.7	72.5	1.1	2.8	2.5
4	7.3	2.1	82.3	3.1	3.1	2.2
5	8.8	1.3	87.4	1.5	0.5	0.6

Fig. 8. (a) SEM cross section and (b) EPMA chemical analysis results in atomic percent of the joint infrared brazed at 970°C for 3 600 s, (c, d) XRD, SEM BEI and EDS chemical analysis results of the cross section at location F in (a), (e, f) XRD, SEM BEI and EDS chemical analysis results of the cross section at location G in (a).

Ti–6Al–4V substrate results in isothermal solidification rather than eutectic solidification of the molten braze, so the region of transformed β-Ti is broadened as the brazing time increased to 600 s and 1 200 s.

(3) For the 3 600 s brazed specimen, Ti_2Cu, Ti_2Ni and transformed β-Ti are vanished from the infrared brazed joint. Because dissolution of the Nb substrate into molten braze becomes prominent with increasing the brazing time, the β-Ti alloyed with Nb is stabilized at room temperature. Additionally, summation of Cu and Ni concentrations in the brazed joint is approximately 5 at%, well below their original concentrations in the braze alloy. The disappearance of transient Ti_2Cu and Ti_2Ni intermetallics for the longer brazing time makes Ti–15Cu–25Ni filler metal with a great potential in future applications.

Acknowledgements

The authors gratefully acknowledge the financial support of this research by National Science Council (NSC), Republic of China under NSC grant 95-2221-E-002-057.

REFERENCES

1) D. W. Liaw and R. K. Shiue: *Metall. Mater. Trans. A*, **36A** (2005), 2415.
2) M. Schwartz: Brazing for the Engineering Technologist, ASM Int., Materials Park, OH, (1995), 147.
3) M. Schwartz: Brazing, ASM Int., Materials Park, OH, (1987).
4) G. Humpston and D. M. Jacobson: Principles of Soldering and Brazing, ASM Int., Materials Park, OH, (1993), 31.
5) D. L. Olson, T. A. Siewert, S. Liu and G. R. Edwards: ASM Handbook, Vol. 6 Welding, Brazing and Soldering, ASM Int., Materials Park, OH, (1993), 941.
6) C. S. Chang and B. Jha: *Weld. J.*, **82** (2003), 28.
7) C. T. Chang, Y. C. Du, R. K. Shiue and C. S. Chang: *Mater. Sci. Eng. A*, **420A** (2006), 155.
8) R. K. Shiue, S. K. Wu and Y. L. Lee: *Intermetallics*, **13** (2005), No. 8, 818.
9) P. Villars, A. Prince and H. Okamoto: Handbook of Ternary Alloy Phase Diagrams, ASM Int., Materials Park, OH, (1995), 9846.
10) R. Roger, E. W. Collings and G. Welsch: Materials Properties Handbook: Titanium Alloys, ASM Int., Materials Park, OH, (1993), 5.
11) T. B. Massalski: Binary Alloy Phase Diagrams, ASM Int., Materials Park, OH, (1990), 2873.
12) S. Krishnamurthy and F. H. Froes: *Int. Mater. Rev.*, **34** (1989), 297.